Neutron reflectivity at the solid/liquid interface: examples of applications in biophysics

2001 J. Phys.: Condens. Matter 13 4973

(http://iopscience.iop.org/0953-8984/13/21/322)

INSTITUTE OF PHYSICS PUBLISHING JOURNAL OF PHYSICS: CONDENSED MATTER

J. Phys.: Condens. Matter **13** (2001) 4973–4989 www.iop.org/Journals/cm PII: S0953-8984(01)20908-4

Neutron reflectivity at the solid/liquid interface: examples of applications in biophysics

Giovanna Fragneto-Cusani

Institut Laue–Langevin, 6 rue Jules Horowitz, BP 156, F-38042 Grenoble, France

Received 15 January 2001

Abstract

Over the last 20 years, neutron reflection has emerged as a powerful technique for investigating inhomogeneities across an interface, inhomogeneities either in composition (Lu and Thomas 1998 *J. Chem. Soc. Faraday Trans.* **94** 995) or magnetization (Felcher 1981 *Phys. Rev.* B **24** 1995). By measuring the reflected over the incoming intensity of a well collimated beam striking at an interface, as a function of the incident angle and wavelength, the concentration profile giving rise to a reflectivity curve is calculated. The success of neutron reflection arises from the fact that, because of the short wavelengths available, it has a resolution of a fraction of a nanometre, so that information is gained at the molecular level. Unlike x-rays it is not destructive and can be used at *buried* interfaces, which are not easily accessible to other techniques, such as liquid/liquid or solid/liquid, as well as at solid/air and liquid/air interfaces. It is particularly useful for soft-matter studies since neutrons are strongly scattered by light atoms like H, C, O and N of which most organic and biological materials are formed. Moreover, the nuclei of different isotopes of the same element scatter neutrons with different amplitude and sometimes, as in the case of protons and deuterons, with opposite phase. This allows the use of the method of *contrast variation*, described below, and different parts of the interface may be highlighted. For biophysics studies, a major advantage of reflectivity over other scattering techniques is that the required sample quantity is very small ($<10^{-6}$ g) and it is therefore suitable for work with expensive or rare macromolecules.

While specular reflection (angle of incoming beam equal to angle of reflected beam) gives information in the direction perpendicular to the interface, the lateral structure of the interface may be probed by the nonspecular scattering measured at reflection angles different from the specular one (Sinha *et al* 1998 *Phys. Rev.* B **38** 2297, Pynn 1992 *Phys. Rev.* B **45** 602). This technique is widely used with x-rays while there are far fewer data in the neutron case due to the smaller intensity of neutron beams. An example relevant in biophysics where the neutron technique has been applied is the off-specular scattering from highly oriented multilamellar phospholipid membranes (Munster *et al* 1999 *Europhys. Lett.* **46** 486).

Neutron reflection is now being used for studies of surface chemistry (surfactants, polymers, lipids, proteins and mixtures adsorbed at liquid/fluid and solid/fluid interfaces), surface magnetism (ultrathin Fe films, magnetic

multilayers, superconductors) and solid films (Langmuir–Blodgett films, thin solid films, multilayers, polymer films). The number of reflectometers in the neutron facilities all around the world is increasing although the use of the technique is not yet very common because the availability of beam time is restricted by cost.

Since many biological processes occur at interfaces, the possibility of using neutron reflection to study structural and kinetic aspects of model as well as real biological systems is of considerable interest. However, the number of such experiments so far performed is small. The reason for this is probably because it is well known that the most effective use of neutron reflection involves extensive deuterium substitution and this is not usually an available option in biological systems. This problem may be partially solved by deuteriating other parts of the interface as described by Fragneto *et al* (2000 *Phys. Chem. Chem. Phys.* **2** 5214).

In this paper we shall concentrate on the use of specular neutron reflection at the solid/liquid interface, less studied than the solid/air or liquid/air interfaces, although technologically more important.

After a brief introduction to the theory and measurement of neutron reflectivity, solid/liquid interfaces both from hydrophilic and hydrophobic solids will be described. Three examples of applications in biophysics will be given:

(1) the adsorption of two proteins, β-casein and β-lactoglobulin, on hydrophobic silicon;
(2) the interaction of the peptide *p-Antp43-58* with phospholipid bilayers deposited on silicon;
(3) the *fluid floating bilayer*, a new model for biological membranes.

(Some figures in this article are in colour only in the electronic version; see `www.iop.org`)

1. An introduction to neutron reflection

1.1. Basic theoretical principles

A full overview of the theory of neutron reflection is beyond the scope of this paper. Complete reviews can be found in [7–10].

There are two possible approaches to the theory of neutron reflection. One involves the demonstration that neutrons behave in the same way as light and the application of standard optics, while the other involves the treatment of neutrons as particles and the solution of the Schroedinger equation directly for the neutron problem. The former option is preferable for the analysis of specular reflection data because of the existence of algorithms to calculate the reflectivity exactly for any structure normal to the surface and the availability of exact and approximate solutions for particular interfacial profiles. For non-specular reflection it is more effective to solve the Schroedinger equation. Lekner [11] has given the most comprehensive treatment of particle and wave reflection. The Schroedinger equation may be written as

$$-\frac{h^2}{8\pi^2 m}\nabla^2\Psi + V\Psi = E\Psi \tag{1}$$

where h is Planck's constant, m is the neutron mass, V is the potential to which the neutron is subject and E its energy. V represents the net effect of the interactions between the neutron and the scatterers in the medium through which it moves. To a good approximation, V is given by

$$V = \frac{h^2}{2\pi m}\rho \tag{2}$$

where ρ is the *scattering length density* (SLD) defined as

$$\rho = \sum_j b_j n_j \tag{3}$$

n_j is the number of nuclei per unit volume and b_j is the scattering length of nucleus j. The latter is an empirical quantity known for most nuclei and the success of most neutron experiments depends on it varying randomly through the periodic table and often varying sharply between isotopes of the same element. For reflection at a planar boundary between air ($V = 0$) and a uniform medium with potential V, the motion of the neutrons through the interface depends only on the potential in the direction normal to the interface, z.

In the neutron problem it is more convenient to think in terms of momentum transfer perpendicular to the interface, q_z, which is given by the change in the neutron wave vector on reflection at the boundary (see figure 1(a))

$$q_z = 2k_i = \frac{4\pi}{\lambda}\sin\theta \tag{4}$$

where λ is the wavelength of the incoming beam and θ the angle of the beam with the interface. It can be shown that the full expression for the reflectivity from a smooth surface is

$$R_f = \left[\frac{q_z - (q_z^2 - q_c^2)^{1/2}}{q_z + (q_z^2 - q_c^2)^{1/2}}\right]^2. \tag{5}$$

R_f denotes the *Fresnel* reflectivity. q_c is the critical value of momentum transfer for total reflection and it is given by

$$q_c = \frac{4\pi}{\lambda}(1 - \cos^2\theta_c)^{1/2} = (16\pi\,\Delta\rho)^{1/2}. \tag{6}$$

θ_c is the critical angle below which the beam is totally reflected and $\Delta\rho$ the scattering length density difference of the incoming medium and substrate. As for light, total reflection may occur when neutrons pass from a medium of lower refractive index to one of higher refractive index. Since the neutron refractive indices of most condensed phases are only slightly less than that of air or vacuum, total external reflection is more commonly observed instead of the total internal reflection experienced with light. The critical angle for total reflection is such that the reflectivity of neutrons of a given wavelength from a bulk interface is unity at lower glancing angles and falls sharply at larger angles.

Many measurements are made at values of q_z much larger than q_c so that

$$R_k \approx \frac{16\pi^2}{q_z^4}\Delta\rho^2 \tag{7}$$

which is the reflectivity in the kinematic approximation. This shows that the reflectivity above the critical angle decreases sharply with q.

For a uniform layer on a substrate the reflectivity is given by

$$R_k \approx \frac{16\pi^2}{q_z^4}[(\rho_1 - \rho_0)^2 + (\rho_2 - \rho_1)^2 + 2(\rho_1 - \rho_0)(\rho_2 - \rho_1)\cos q_z d] \tag{8}$$

where d is the thickness of the layer and ρ_1, ρ_2, ρ_0 are the scattering length density of the layer and two bulk phases. Below q_c, R is unity and the reflectivity profile does not contain any

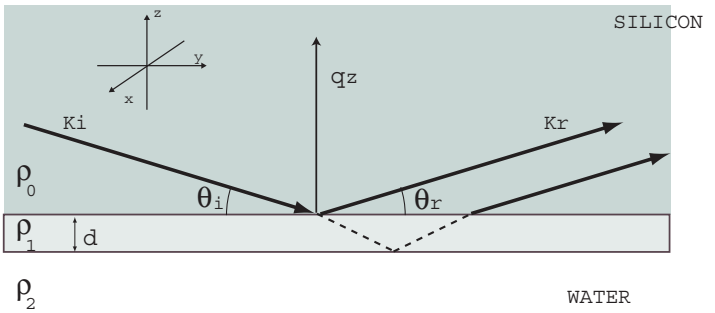

(a)

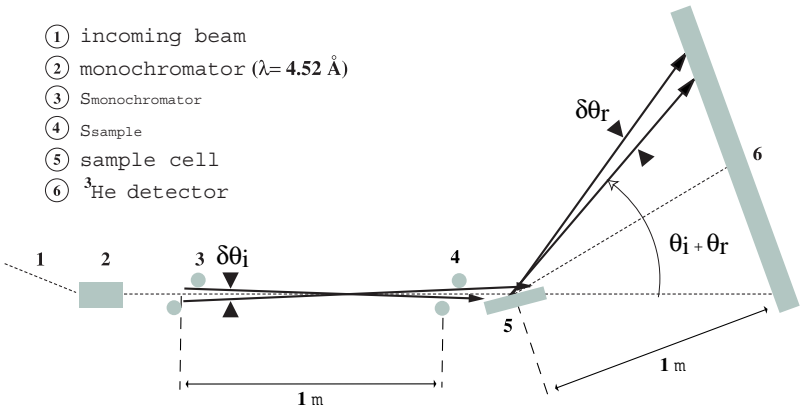

(b)

Figure 1. (a) Reflection of an incident beam from two flat interfaces; k_i and k_r are the incident and reflected wave vectors; q_z is the component of the momentum transfer perpendicular to the interface. See the text for details. (b) Layout of the diffractometer D16 at the ILL as used for reflectivity experiments, see [30] for details.

structural information about the layer. Above q_c, R has maxima and minima and the separation of the maxima is $2\pi/d$. The method of calculating the Fresnel reflection may be extended to systems with more than one layer at the interface, although for a system of more than four layers the calculation becomes cumbersome. The interface roughness may be included by modelling the reflectivity with a Debye–Waller type factor, derived from a Gaussian height distribution factor [12].

Born and Wolf give a general solution, the so called *optical matrix method* [13], to calculate the reflectivity from any number of parallel, homogeneous layers, which is particularly useful since any layer structure can be approximately described by dividing it into an arbitrary number of layers parallel to the interface, each having a uniform scattering length density. Such layers do not need to have identical thickness. Since the reflection of neutrons is identical to the reflection of electromagnetic radiation polarized perpendicular to the reflection plane, by using the condition that the wave function and its derivative must be continuous at each boundary, the neutron reflectivity profile can be calculated by determining a characteristic matrix from the solution to the Maxwell equations for each

layer and then multiplying the characteristic matrices to give the reflectivity amplitude matrix.

1.2. The measurement of neutron reflectivity

The basic features of a reflection experiment, whether this uses light, x-rays or neutrons, are (i) a radiation source, (ii) a wavelength selector (or chopper(s)) (iii) a system of collimation, (iii) the sample and (iv) a detection system (see figure 1(b)).

The production of neutrons requires either a nuclear reactor, where a continuous neutron beam is produced by nuclear fission, or a pulsed source, where a pulsed beam is obtained when a burst of high-energy protons or electrons from a particle accelerator hits a heavy nucleus. In both cases neutron energies are too high for structural or dynamical studies and are reduced in a moderator tank where the neutrons are repeatedly scattered losing energy at each collision until thermal equilibrium is reached. Thermal neutron energies are of the order of $k_B T$ where T is the temperature of the water moderator and k_B the Boltzmann constant. Neutrons can interact with nuclei via nuclear forces or with the magnetic moment of unpaired electrons. This review will be confined to nuclear interactions.

1.3. Neutron reflectometers

The objective of a specular neutron reflection experiment is to measure the reflectivity as a function of the wave vector perpendicular to the reflecting surface, q_z. From the definition of q_z (see equation (4)) it follows that the measurement can be made by varying either or both the glancing angle of incidence θ and the neutron wavelength λ. In most nuclear reactors measurements are usually made at a fixed value of λ using long wavelength neutrons and a θ (reflection angle)–2θ (detector angle) scan. Wavelength selection may be achieved by Bragg scattering from a crystal monochromator or by velocity selection through a mechanical chopper. The resolution in such measurements is determined by both angular, $\Delta\theta$, and wavelength, $\Delta\lambda$, spread. At spallation sources time-of-flight instruments (TOF) operate at fixed θ and the range of momentum transfer results from the different wavelengths that comprise a polychromatic neutron beam. The values of q are determined from the time of arrival of each neutron as a function of its wavelength, the shorter wavelengths neutrons arriving first, so that each pulse gives information over the whole q range. The relative resolution $\Delta q/q$ is dominated by the angular divergence $\Delta\theta$ of the beam and is therefore constant over the measurement of the reflectivity profile. However the actual resolution Δq varies widely over the whole range.

Measurements of neutron reflectivity can be made on dedicated reflectometers or on diffractometers and triple-axis spectrometers where it is possible to do a θ–2θ scan. Among the reflectometers where work on biophysics systems has been done in the past are *Ng1* and *Ng7* at the reactor of the National Institute of Standard and Technology (NIST) in the USA, *CRISP* and *SURF* at the ISIS spallation source of the Rutherford Appleton Laboratory (RAL) in the UK and the diffractometer *D16* and the former triple-axis spectrometer *D17* at the reactor of the Institut Laue Langevin (ILL) in France. All these instruments have been described in detail elsewhere [14–19].

D17 has been recently rebuilt and it has become a dedicated reflectometer working both in monochromatic and TOF modes. It is the most powerful and versatile reflectometer in the world because of its high flux in the monochromatic mode and flexible resolution in the TOF mode ($\Delta q/q = 0.001$–0.2). It is an instrument with great potential for soft matter studies where high flux and high signal/noise are desired and kinetics studies are relevant. Its multidetector is particularly useful for off-specular measurements and, again, this is a valuable feature for

biophysics studies since off-specular scattering arises from lateral inhomogeneities, which are common in biological systems. An example of data from D17 is shown in figure 5(b) [20].

1.4. Background subtraction

As q_z increases the noise level increases since not all the neutrons detected are from specular reflection. At high values of q_z the reflectivity is very small and most of the beam passes into the subphase (e.g. water) where it is scattered either incoherently or by multiple diffraction. A proportion of this scattering enters the detector with the specular reflection and contributes a background, which has to be subtracted from the profile. There are other sources of background related to the environment of the sample and the components of the reflectometer, although the incoherent scattering from the sample itself is the major source. Incoherent scattering comprises a number of scattering events which are completely random and arise because not all nuclei of a given element are identical either because of different isotopes or because of different nuclear spin states. Such scattering is isotropic.

The principle of background subtraction is the same in every reflectometer. On zero or one-dimensional detectors, the off specular scattering at each incident angle is measured and subtracted from the profile. This may be done by rotating the detector to higher and lower angles, averaging the two measurements and subtracting the resulting profile from the reflectivity. This procedure is used on Ng7, CRISP and SURF. On D16 and D17 the same principle is followed, although the calculation is different. The area of the full specular peak on the position sensitive detector, x, is chosen and integration gives the total number of counts, n_x. Repeating the summation over a larger area, y, still centred on the reflected peak, a value n_y is obtained. The difference in the number of counts divided by the difference in the area gives the number of background counts per unit area of the detector around the reflected peak. The number of background counts in the region of the reflected peak is then $[x(n_x - n_y)/(x - y)]$.

For solid/liquid samples the background is high because of the incoherent scattering of the liquid and the scattering from Teflon and aluminium from the cell (figure 2) and usually a maximum of six orders of magnitude in reflectivity are measured. Majkrzak *et al* [21] have succeeded in attaining lower reflectivities with a special cell set-up and measuring times of >15 hours on the reflectometer Ng1 at NIST.

1.5. Data analysis

The method of analysis often used for specular reflection data involves the construction of a model of the interface that may be represented by a series of parallel layers of homogeneous material. Each layer is characterized by a scattering length density, ρ, and a thickness, d, which are used to calculate a model reflectivity profile by means of the optical matrix method described above. The interfacial roughness between any two consecutive layers, σ, may also be included in the model by the Abeles method [22]. The calculated profile is compared to the measured profile and the quality of the fit is assessed either visually or by using χ^2 in the least-squares method. In a solid/liquid experiment the solid medium and the liquid solution are considered as having infinite thickness and have a fixed scattering length density. The adsorbate may form a single layer or a more complicated structure on the surface. By variation of ρ and d for each layer, the calculated profile may be compared with the measured profile until the optimum fit to the data is found. Although any one profile may not provide a unique solution, the use of different isotopic contrasts together with the physical and chemical constraints of the system can usually ensure that an unambiguous model of the interface is obtained. *Contrast variation* relies on the fact that the different nuclei scatter neutrons with different amplitude,

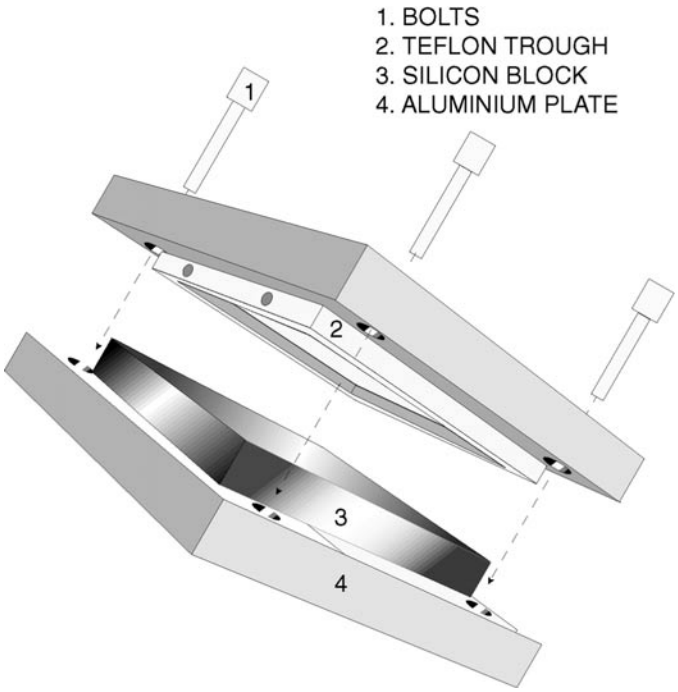

Figure 2. Typical cell used for reflectivity measurements at the solid/liquid interface.

and sometimes, as in the case of protons and deuterons, with opposite phase. By using a combination of hydrogenated and deuteriated materials the reflectivity profile of a system can be substantially changed while keeping the same chemical structure at the interface. It is also possible, by adjustment of the H/D ratio, to prepare solvents which are contrast matched to the medium through which neutrons pass before reaching the interface, that is the bulk solid in a solid/fluid experiment or air in a liquid/air experiment. The contrast between the solid (or air) and the solvent is then zero, giving a reflectivity profile arising only from the interfacial region. From the value of the scattering length density of the layer information about its composition is obtained. Our experience is that at silicon/water interface measurements from the same layer should be done in four water contrasts with scattering length densities in roughly arithmetical progression, 0/2/4/6. The water contrasts are then: (i) H_2O, neutron scattering length density of -0.56×10^{-6} Å^{-2}; (ii) SMW (*silicon-matched water*), a mixture of H_2O and D_2O with the same refraction index for neutrons as bulk silicon, that is scattering length density of 2.07×10^{-6} Å^{-2}; (iii) 4MW, a mixture of H_2O and D_2O with neutron scattering length density of 4×10^{-6} Å^{-2}; (iv) D_2O, neutron scattering length density of 6.35×10^{-6} Å^{-2}.

The kinematic approximation [23] gives a more direct description of the structure of soluble surfactant monolayers at the air/liquid interface. Very recently, Majkrzak *et al* [21] have succeeded in applying a new, phase-sensitive method to reveal compositional depth profiles. With this method the scattering length density profile of biomimetic membranes is obtained by a first principles inversion without the need for fitting or adjustable parameters. Other model-free approaches use maximum entropy [24] and B splines [25].

2. Solid/liquid samples

Liquids diffract strongly neutrons over a continuous range of angles and are not sufficiently transparent for the normal configuration in solid/liquid experiments. On the other hand diffraction from a solid can be avoided either by a suitable orientation of a single crystal or by choosing an incoming wavelength above the Bragg cut-off. Since solids of large size are required only a few solids are available at an accessible price. The solids most often used are silicon and quartz. For silicon, there are well established methods for making reproducible hydrophobic coatings. The simplest procedure is to graft a layer of hydrocarbon chains on to the natural oxide surface by self-assembly, for example by the reaction of alkyl chlorosilanes (see below).

The size of the samples used in neutron reflection experiments depends on the resolution required. If reflectivity values at high q are important the sample must be as large as possible (typically more than 50 mm long and 30–50 mm wide). For high $\Delta q/q$ resolution or where the reflectivity is well above the background, a smaller illuminated area can be used, down to 15×10 mm^2. For thin adsorbed layers, for which the reflectivity at high values of q contains most of the structural information, large samples are necessary. In order to ensure flatness thick solid samples are also preferred (10–25 mm). An example of solid/liquid cell is shown in figure 2. The cell consists of a silicon crystal clamped against a PTFE trough with a capacity varying between 10 and 30 cm^3. The trough is filled with solution through two filling ports and sealed using two PTFE stoppers. The whole assembly is bolted on aluminium plates and mounted on the goniometer of the reflectometer. The large face of the silicon block is aligned along the axis of the neutron beam.

Before the characterization of the layers at the interface, it is desirable to have *well defined, reproducible and clean surfaces*. The surfaces of solids are very complex and their nature and properties depend largely on the past history of exposure to various physical and chemical conditions. With the exceptions of freshly cleaved mica, surfaces are rough on various length scales and contain steps, ledges or dislocations. In addition, they are usually chemically different from the bulk solid because of oxidation, diffusion of impurities from the bulk or contamination. These effects may cause the interactions between amphiphiles and solid surfaces to be irreproducible and therefore care must be taken to minimize their impact.

2.1. The surface of silicon

When clean silicon surfaces are exposed to the atmosphere at room temperature, they rapidly become coated with a thin layer of silica referred to as *native oxide*, its composition being approximately that of a silicon oxide, SiO_2. The nature of the silica layer on silicon crystals is not yet fully understood and varies depending on the condition of growth of the oxide and the lattice structure of the surface. Most studies have shown that this layer consists of an amorphous material with a thickness ranging from 10 to 30 Å. The surface chemistry of silicon after exposure to air may be treated as though it is the surface of silica. Whatever its underlying composition, the characteristic of the siloxane Si–O–Si surface of SiO_2 is that the residual valences react with water so that at ordinary temperatures the surface becomes covered with silanol groups, Si–OH. Since the silicon atoms on the surface are not in regular geometrical order, the hydroxyl groups are not equidistant from each other and their chemical behaviour is different [26].

Once a silicon crystal is grown, the flatness and smoothness of its surface is ensured by *polishing* the surface. This essentially consists of rubbing and dissolving layers of it with small particles and under pressure. The final step, before the experiment, will be the cleaning from organic and inorganic impurities accumulated during the storage. A review of methods used to

clean silicon surfaces can be found in [27]. We have found that irradiating a surface with short wavelength UV from a mercury quartz lamp in the presence of oxygen is a powerful technique for removing many contaminants [28]. Oxygen absorbs 185 nm radiation forming very active ozone and atomic oxygen. The technique is suitable for removal of organic contaminants but is not effective for most inorganics or metals. The treatment consists of irradiating freshly polished blocks with UV light under a constant flow of oxygen for a time depending on the size of the surface and its closeness to the lamp, for our samples the treatment lasts about half an hour.

Both in the case of adsorption from solution and for lipid deposition it is important to have a surface as smooth as possible. It has been shown [29] that the roughness of the surface has a significant effect on the properties of a cationic surfactant layer. On a rough surface (roughness $\sim$14 Å) a surfactant bilayer forms which is thicker than the one formed on a smoother surface (roughness $\sim$6 Å) and unsymmetrical in the direction of the surface normal. The surface coverage was also found to be 15% lower on the rough surface. For lipid depositions a smoother surface leads to higher transfer ratios [30].

2.2. Hydrophobic silicon: self-assembled monolayers

Back in 1891 Agnes Pockels [31] first produced organic monolayers on the surface of water by compressing soap films using an apparatus that was a forerunner of the more famous Langmuir trough. Much work has been devoted since to the study of films at the water interface but only relatively recently large organic molecules have been found to assemble onto surfaces of solids to form monolayers with a high degree of structural order. These self-assembled monolayers (SAMs) are chemisorbed to the surface and present lateral interactions (usually van der Waals) between the molecules, which lead to densely packed, and usually crystalline monolayer structures [32, 33]. Besides being very stable (they can last unchanged for months), SAMs are very flexible since a great variety of structures may be created by varying the length of the alkyl chain or the functional group at its end, by coadsorbing two or more molecules and by chemical or photochemical reactions in the preformed monolayers. The understanding of the roles played by the intermolecular and molecule–surface interactions in controlling the structure and properties of the monolayer is seen as an important step for the understanding of more complex systems such as membranes and micelles and this, together with the fact that SAMs are ideal model systems for the study of interfacial phenomena like wetting, adhesion, friction, corrosion and electron transfer, has caused many research groups around the world to study such systems. The most common SAMs are alkanethiols on gold and alkyl silanes on silicon. For reflectivity studies silanes are more convenient because monolayers can be assembled directly on silicon crystals. Krueger *et al* ([34] and references therein) have done much work by depositing a thin layer of gold on silicon and forming a self-assembled monolayer from alkanethiol used as substrate to support lipid bilayers. This system is complicated by the presence of the gold layer that must be taken into account in the analysis of the composition at the interface.

Octadecyl trichlorosilane, commonly known as OTS, is the most common organochloro silane used for the formation of self-assembled monolayers on oxidized silicon and glass solids. Its success arises in part from the ability of the trichlorosilyl head group to react with hydroxyls on the solid surface to form siloxy bonds. The hydrocarbon film is therefore chemisorbed at the surface with densely packed chains in extended conformation, which are oriented nearly perpendicular to the surface. The film is characterized by a remarkable physical and chemical stability. Since silicon is the most common solid for neutron reflectivity

experiments, hydrophobic layers from OTS are widely used when this technique is needed for adsorption studies at hydrophobic surfaces.

The presence of an oxide and a hydrophobic layer on the solid medium greatly complicates the analysis of neutron reflectivity data from adsorbed layers with respect to similar analyses of data from the air/water interface. These two additional layers must be characterized before the adsorption process because any errors in their structural parameters may make it either impossible to find a model, or lead to an incorrect model, of the adsorbed layer. A discussion of how the deuteriation of OTS layers on silicon may help in the study of macromolecules difficult to deuteriate is given in [6].

3. Examples of applications

3.1. Adsorption of proteins at the solid/liquid surface

Many proteins are amphiphilic because they contain a mixture of amino acids with hydrophobic chains and with ionic or polar side chains. They aggregate in solution and may be surface active even at very low concentrations. The mechanism of adsorption and the structure of the adsorbed protein layers are important pieces of information in areas relevant to biology (protein chromatography, cellular adhesion) [35], medicine (biomedical materials) [36], food processing (stabilization of foams and emulsions, fouling of equipment) [37] and biotechnology [38], and therefore considerable effort has been devoted to studying what are the important factors, which will include size, shape, charge, hydrophobicity, thermodynamic and thermal stability. There is no comprehensive model of protein adsorption, although a large number of studies of protein adsorption at various surfaces have been made, such as colloidal particles, metal surfaces, silica surfaces, modified silicon surfaces, polymer surfaces and air–liquid interfaces.

The nature of the surface has a strong effect on the structure and composition of the protein layer so that it is difficult to construct theoretical models and it is desirable to work with well defined interfaces. A strong interaction between proteins and a surface often leads to irreversible adsorption and protein denaturation. In order to understand protein adsorption it is important the *in situ* determination of the protein structure at the interface. Classical techniques such as IR, NMR, circular dichroism, ellipsometry, electophoresis and others have been used to investigate protein adsorption on flat surfaces but none of them can give direct determination of the structure at the interface. Neutron reflection represents a powerful tool for the direct determination of both low-resolution structure and composition of the adsorbed layer [39–41].

Our example concerns the two proteins β-casein (β-CN) and β-lactoglobulin (β-Lg) adsorbed on deuteriated OTS self-assembled monolayers on silicon at pH 8, 7, 5 and 3 from water solutions of different isotopic composition (see, for example, figure 3(a)) [6, 40]. At pH 7 β-CN reflectivity profiles are consistent with a two layer model: a more compact layer adjacent to the surface of thickness 30 ± 3 Å and volume fraction 0.62 and a looser and thicker layer protruding into the solution of thickness 65 ± 5 Å (see the cartoon in figure 3(b)) and volume fraction 0.20. For the globular β-Lg at pH 7 a one layer model was required to fit the adsorbed protein layer and this was expected because of its more compact structure in solution. The thickness, 32 ± 4 Å, is slightly lower than the diameter of the protein in solution (36 Å), which is not surprising since the protein may be forced to flatten somewhat for better contact with the surface. At values of pH different from 7, both proteins show more adsorption and thicker layers. β-Lg now adsorbs in two layers and this may be explained by assuming either that the protein unfolds, and this has been suggested by other authors who have investigated its

secondary structure, or that it aggregates. It is believed that a compact globular molecule does not generally unfold to such an extent that it forms an adsorbed layer with loose loops and tails so that the formation of aggregates (additional layers on top of the first) seems more likely. During this study it was found that a mixture of D_2O and H_2O of scattering length density 4.5×10^{-6} Å^{-2} (water$_{4.5}$) is more sensitive to the larger scale thickness of the adsorbed layers than D_2O (which gives a bigger contrast to the proteins). In fact, the largest scale dimensions in the protein have their main effect at low angles where they are masked by the higher critical angle of D_2O and this detail is only revealed in water$_{4.5}$.

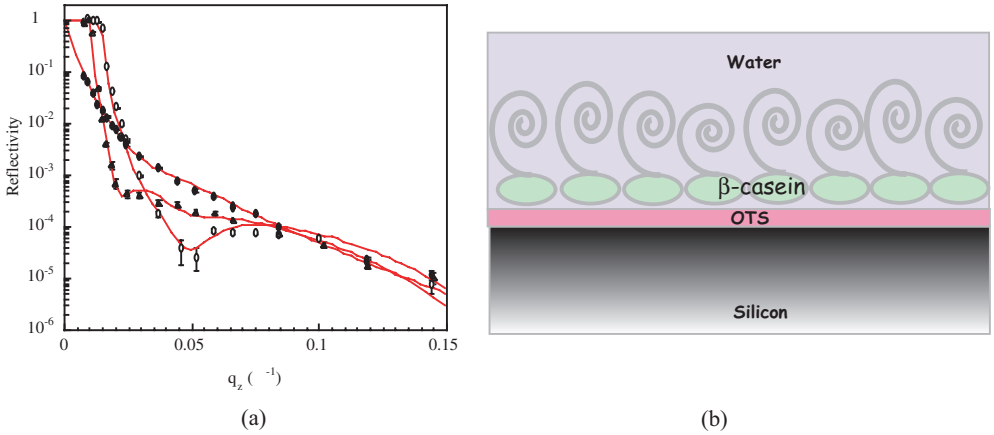

(a) (b)

Figure 3. (a) Neutron reflectivity profiles (points) and best fits (continuous lines) measured from β-casein adsorbed at pH = 7 on deuteriated OTS in (○) D_2O, (●) H_2O and (▲) water with an SLD $= 4.5 \times 10^{-6}$ Å^{-2}: for details see [6]. (b) Schematic representation of an adsorbed layer of β-casein at the interface between a modified hydrophobic silicon surface and an aqueous solution. Measurements were made on D17 *before* rebuilding (ILL).

The adsorption of both proteins was found to be irreversible although they could be removed by a dilute solution of pure non-ionic surfactant.

3.2. Interaction of a peptide with phospholipid bilayers

Lipid bilayers are the basic building units of biological membranes. Many biological processes involve transformations between such bilayer structures. Several model membrane systems have been developed for studying the properties of pure lipids, lipid mixtures and lipid–protein mixtures and they can be grouped as (i) monolayers, (ii) planar bilayers and (iii) liposomes or vesicles. In this review we shall limit the discussion to the planar bilayers on solid supports.

Phospholipid bilayers have been intensely used as model systems for studying the structure and interactions of biological membranes [42, 43]. In the study presented here, neutron reflectivity has been used to study the structure of deposited phospholipid bilayers in the gel phase and the modifications induced by the presence of a 16 amino-acid peptide, the third helix of the Antennapedia homeodomain, *p-Antp43-58* [44]. p-Antp43-58, and some of its analogues [45, 46], can translocate across neural cell membranes, without destroying them, through a likely non-specific interaction with the lipids of the membrane. The experiments carried out on this system tend to exclude all classical mechanisms of cell insertion: the translocation across the plasma membrane does not require specific receptors or a helix conformation; internalization occurs both at 4 °C and at 37 °C and the mechanism is likely to be different from classical endocytosis. In order to understand the mechanism of interaction of the peptide

with the membrane, this was modelled with a phospholipid bilayer deposited on the highly hydrophilic surface of a silicon(111) crystal. The main interest of such a model, besides allowing reflectivity measurements, is that the bilayer can be studied in bulk water and a stable, unique, bilayer can be looked at.

The phospholipids were di-palmitoyl phosphatidyl-choline (DPPC) and mixtures of DPPC with 10% mol:mol of the negatively charged di-palmitoyl phosphatidyl-serine (DPPS). They were deposited on silicon single crystals by using a combination of the Langmuir–Blodgett (first layer) and Langmuir–Schaeffer (second layer) techniques [47]. Briefly, after spreading a phospholipid monolayer on the surface of water, at a pressure <0.1 mN m^{-1}, and allowing for the evaporation of the solvent, the monolayer was compressed to a surface pressure of 30 mN/m and the highly hydrophilic block (a silicon crystal previously cleaned with organic solvents and UV/ozone treatment) was immersed in the subphase. By withdrawing the block from water, at a speed of 5 mm min^{-1}, a monolayer of lipid was deposited on its surface. The solid was then rotated by 90° and slowly reimmersed with the large face parallel to the water surface for the formation of the bilayer. The pressure was kept constant all the time. Stable and reproducible bilayers were obtained. Neutron reflectivity was measured from both hydrogenated and deuteriated lipids in four water contrasts. Measurements were taken first from the bilayers alone and then from bilayers containing the peptide (see, for example, figures 4(a) and 4(b)) [44]. By pushing the resolution of neutron reflectivity measurements [44], the bilayer structure was determined at one Ångstrom precision (see figure 4(c)). The thickness of the thin water layer between the solid and the phospholipids was found to be 5 ± 1 Å, that of the headgroups 9 ± 1 Å and that of the chains 36 ± 1 Å. The deposited bilayer had the same roughness, 5 ± 1 Å, as the silicon itself. Our results on the bilayer structure agree with literature data on phospholipid bilayers and stacked bilayers but greater details are given on the structure and composition. The chain thickness (36 ± 1 Å) is smaller than the length of two fully extended lipid chains. This means that chains either intermix or, more likely, they are tilted 39° from the normal. In order to explain the origin of the percentage of water (15 to 20%) in the bilayer necessary to fit the data it is suggested that the bilayer covers about 80% of the available surface. Neutron specular reflection gives no information about the in-plane structure at the interface and therefore it is not possible to determine whether the water is uniformly distributed among the lipids or whether it concentrates in holes of the bilayer. A preliminary analysis of synchrotron radiation off specular measurements on these samples suggests that the bilayer contains about 15% of holes of 6 nm diameter [48]: this result needs to be confirmed by further analysis.

After introduction of *p-Antp43-58*, the bilayer structure becomes more complicated. There are more unknown parameters; the uncertainty in the thickness increases but is not larger than 2 Å. In the presence of zwitterionic lipids (DPPC), the structure of the bilayer is maintained, in terms of thickness and roughness, while changes in the scattering length density are consistent with an incorporation of peptide either segregated in holes of the bilayer or uniformly distributed in the membrane. Since incorporation inside the membrane is likely to perturb its thickness and/or roughness, we suggest that the peptide be segregated in the holes.

When peptide is added in the presence of 10% mol:mol negatively charged lipids (DPPS), the structure is modified. The most remarkable effect of the presence of peptide in the membrane is the significant increase of the roughness from 6 ± 1 Å, in the bare bilayer (which is roughly the same as the silicon surface), to 13 ± 2 Å in the bilayer + peptide. It is suggested, from the model used to analyse data, that it is mainly segregated into the outer boxes (figure 4(d)). Deuterated peptide would be more helpful for these determinations since it is found that the protonated one has SLD similar to that of the protonated headgroups, but the compound is not yet available. A more precise indication of the position of the peptide

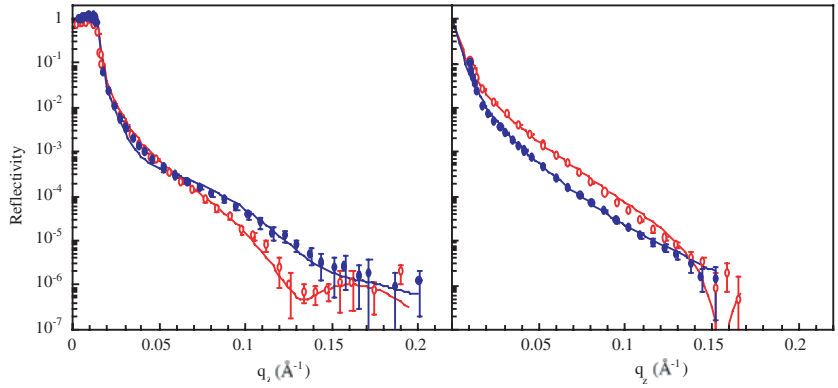

(a) (b)

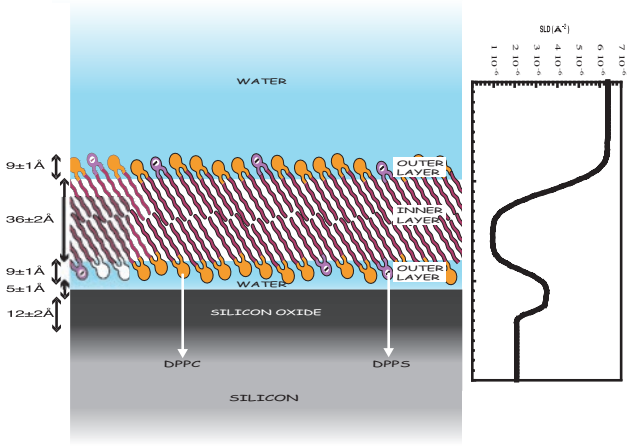

(c)

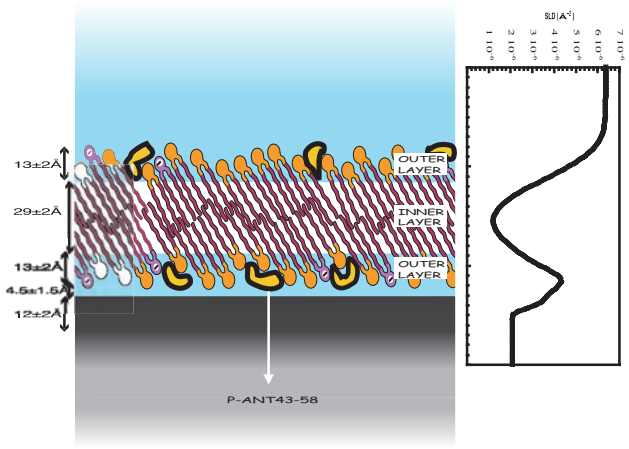

(d)

Figure 4. Neutron reflectivity profiles (points) and fitted curves (continuous lines) from (○) hydrogenated DPPC+10% DPPS deposited on silicon and (●) same lipid composition codeposited with *p-Ant*$_{43\text{-}58}$ in (a) D_2O and (b) H_2O. Cartoon and density profile in D_2O for (c) the bilayer alone and (d) the peptide containing bilayer. For details see text and [44]. Measurements were made on D16 (ILL).

should also be possible through fluctuation correlations in the plane determined by off-specular reflectivity (work in progress).

Finally, it was shown that neutron reflectivity is a suitable technique for studying the interaction of small molecules, like peptides, with phospholipid single bilayers. The effect of negative charges on the interaction was visible. The deposited bilayer, with and without peptide, was found to be stable in time and the deposition technique very reproducible.

Although the experiment was successful as the effect of the peptide on the bilayer was visible, the biological relevance of the study was limited by the fact that the lipids were in the gel phase. The initial aim was to verify whether there was any affinity of the peptide with the hydrocarbon chains. We have shown that it is not the case. Our current research is directed towards the study of a more relevant model for the membranes, that is a freely floating bilayer, described below.

3.3. Fluid floating bilayers: a new model for membranes

Double lipid bilayers [30, 49] were prepared according to the classical Langmuir–Blodgett deposition on a vertical substrate for the first three layers and a Langmuir–Schaeffer configuration for the fourth layer (see figure 5(a)). This results in the formation of an adsorbed and a floating bilayer.

The floating bilayer at the solid–liquid interface is a new model for biological membranes with several advantages over classical model systems. It is more hydrated than adsorbed single bilayers, since it is separated from the adsorbed one by a 15–30 Å thick film of water (depending on lipid composition and temperature). It is thus more flexible and fluctuating, as evidenced by off-specular synchrotron radiation measurements (work in progress). It is more homogeneous and reproducible than bilayers adsorbed from vesicles at the solid–liquid interface and composition can be varied during preparation so that, for example, asymmetric bilayers can be prepared. It has the same ordered structure as a single bilayer deposited from a Langmuir monolayer. It is relatively easy to make with a standard Langmuir–Blodgett trough. A clean environment is preferable, but no control of the atmosphere or temperature is strictly necessary. Double bilayers resist manipulation, transport and storage for days as long as they are kept in contact with water. With respect to multilamellar systems, they have a well known position defined by the substrate. This makes possible studies with local investigation techniques. They do not contain any spurious solvent or meniscus.

Phospholipid bilayers exhibit a main phase transition from a gel phase, where lipid chains are rigid and well ordered, to a liquid crystalline phase (L_α), where chains are disordered and fluid-like. Double bilayers are best deposited in the gel phase. After deposition the temperature of the system may be raised in order to overcome the gel–fluid phase transition. This was done both for DSPC and DPPC and very interestingly it was found that the bilayer is stable well above the main transition temperature (in the fluid phase) and that at the transition both the interbilayer distance and the roughness increase. Figure 5(b) shows a neutron reflectivity measurement from hydrogenated DSPC in D_2O at 59 °C (that is, in the fluid phase) taken on D17 after it was rebuilt. In the top right inset there is the variation in inter-bilayer distance (water thickness) around the phase transition and in the bottom left inset is the density profile as from the model used to fit the data (a box model was used and reflectivity determined with the optical matrix method). As observed in the inset the increase in inter-bilayer distance persists over a certain range of temperatures around the phase transition. In fact it is possible that the pre-transition (transition to the ripple phase, L_β), that differential scanning calorimetry studies [50] determine for DSPC at 52 °C is observed and the structure is maintained up to the main transition (55 °C). This same behaviour was

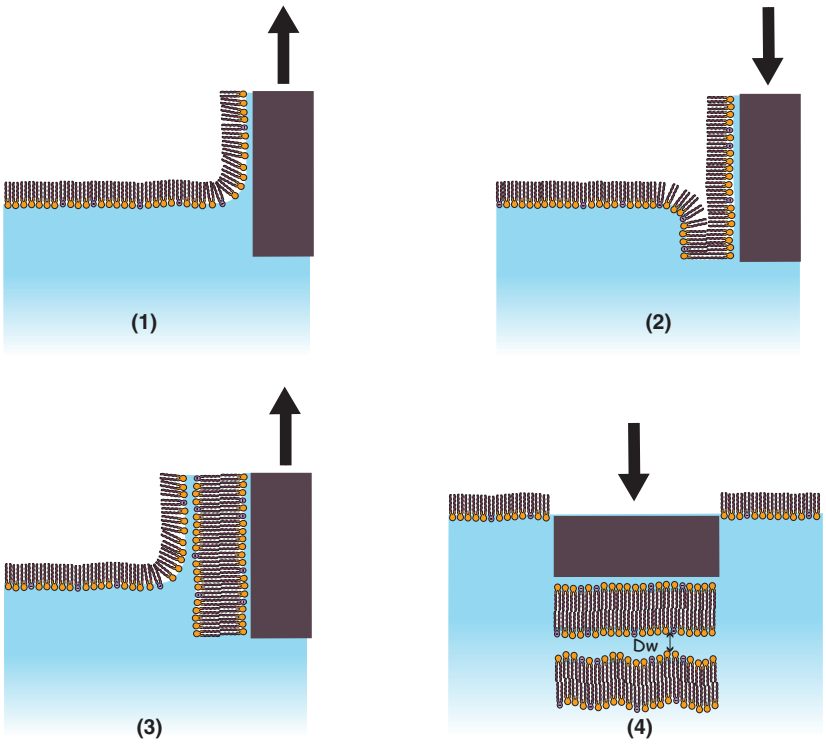

(a)

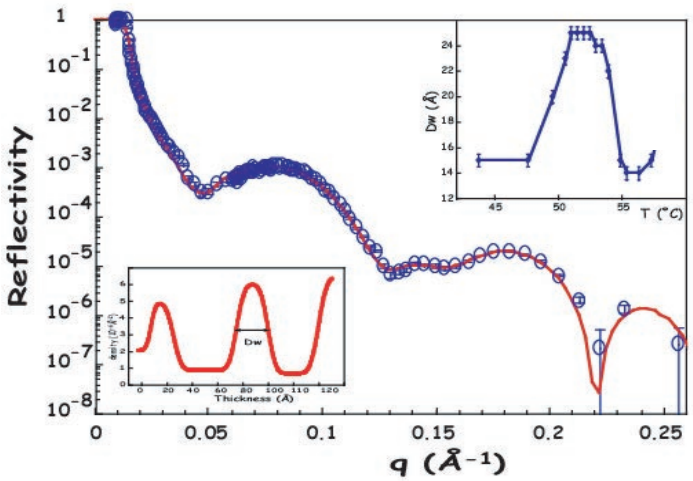

(b)

Figure 5. (a) Cartoon showing the four-step deposition of a double bilayer. Layers 1, 2 and 3 are deposited by the Langmuir–Blodgett method; layer 4 is deposited by the Langmuir–Schaeffer method. See [30] for further details. (b) Neutron reflectivity profile and fitted curve for a hydrogenated DSPC double bilayer in D_2O at 59 °C. Top right inset: variation of the inter-bilayer distance (Dw) with temperature; bottom left inset: density profile from fitted curve. For further details see [20] and [49]. Measurements were made on D17 *after* rebuilding.

observed for deuterated lipids, although in a different temperature range, as the transition for deuterated lipids happens at a different temperature than for hydrogenated ones, and for *DPPC* (work in progress). Another group has observed the swelling at the transition for a floating DMPC bilayer as well [51]. In one case [49] the increase was really spectacular, the thickness of the water layer raising from 16 Å to more than 60 Å. Although we were not able to reproduce this effect, after the experiment, a theoretical treatment was developed which suggests that the giant increase of both thickness and roughness at the transition (i.e. where the bilayer is extremely flexible) might be the first direct observation of the fluctuation-induced repulsion predicted by Helfrich [52] using entropy arguments and considered a key ingredient of bilayer–bilayer interactions. An equation is found to relate the inter-bilayer thickness with the floating bilayer roughness and it describes well all data obtained so far from those systems [49, 53].

4. Conclusions and perspectives

Neutron reflectivity is already a well established technique for the study of nanometre size material at interfaces and since processes at interfaces are important in biology it is a technique with great potentialities for life sciences studies. Advantages over other techniques include the fact that it is non-destructive, it can be used to study *in situ* processes and *buried* interfaces. Although much work has been done in the past on surfactant and polymer layers, the study of biophysics systems is more recent. Here we have given only three examples of applications; many others are possible. In the first example it has been shown that the low-resolution structure at interfaces of proteins can be determined in some detail and the signal may be enhanced, if a deuterated protein is not available, by deuterating the agent used to make the surface hydrophobic. As for the second example, it has been shown that even a very small peptide may be identified in a model phospholipid membrane when this perturbs the structure of the membrane. For the third example neutron reflectivity showed particularly useful for determining structural modifications of lipid bilayers undergoing phase transitions.

Lateral inhomogeneities cannot be probed by specular reflection and off-specular studies become necessary. Much effort has been put recently into the optimization of data analysis from off-specular measurements and in this direction are to be sought the future achievements of the technique as well as in new data analysis methods.

The liquid/liquid interface deserves a special mention for its technological importance as well as its fundamental interest. As far as biological systems are concerned it is interesting because it would allow, for example, the study of translocation of molecules from two liquid mediums through a membrane. Interesting work has been done recently from a phospholipid monolayer at a water/oil interface by using synchrotron radiation [54]. It is more difficult to use neutrons since when the beam crosses one of the two liquid phases to reach the interface, adsorption lowers considerably the signal. Nevertheless, the optimization of sample preparation and data collection protocols could lead to useful results in the near future.

Acknowledgments

The author wishes to thank all of her past and present collaborators and in particular E Bellet-Amalric, T Charitat, R Cubitt, F Graner, A R Rennie and R K Thomas.

References

[1] Lu J R and Thomas R K 1998 *J. Chem. Soc. Faraday Trans.* **94** 995

[2] Felcher G P 1981 *Phys. Rev.* B **24** 1995
[3] Sinha S K, Sirota E B, Garoff S and Stanley H B 1998 *Phys. Rev.* B **38** 2297
[4] Pynn R 1992 *Phys. Rev.* B **45** 602
[5] Munster C, Salditt T, Vogel M, Siebrecht R and Peisl J 1999 *Europhys. Lett.* **46** 486
[6] Fragneto G, Su T J, Lu J R, Thomas R K and Rennie A R 2000 *Phys. Chem. Chem. Phys.* **2** 5214
[7] Daillant J and Gibaud A 1999 *X-ray and Neutron Reflectivity: Principles and Applications* (Berlin: Springer)
[8] Penfold J and Thomas R K 1990 *J. Phys.: Condens. Matter* **2** 1369
[9] Russell T P 1980 *Mater. Sci. Rep.* **5** 171
[10] Zhou X-L and Chen S-H 1995 *Phys. Rep.* **257** 223
[11] Lekner J 1987 *Theory of Reflection* (Dordrecht: Martinus Nijhoff)
[12] Névot L and Croce P 1990 *Revue Phys. Appl.* **15** 761
[13] Born M and Wolfe E 1989 *Principles of Optics* (Oxford: Pergamon)
[14] Dura J A, Richter C A, Majkrzak C F and Nguyen N V 1998 *Appl. Phys. Lett.* **73** 2131
[15] http://www.ncnr.nist.gov/instrument.html
[16] Penfold J, Ward R C and Williams W G 1987 *J. Phys. E: Sci. Instrum.* **20** 1411
[17] Penfold J *et al* 1997 *J. Chem. Soc. Faraday Trans.* **93** 3899
[18] http://www.ill.fr/Yellowbook/D16
[19] http://www.ill.fr/Yellowbook/D17
[20] Cubitt R 2000 *ILL Annual Report*
[21] Majkrzak C F, Berk N F, Krueger S, Dura J A, Tarek M, Tobias D, Silin V, Meuse C W, Woodward J and Plant A L 2000 *Biophys. J.* **79** 3330
[22] Heavens O S 1955 *Optical Properties of Thin Films* (London: Butterworths)
[23] Crowley T L 1993 *Physica* A **195** 354
[24] Silvia D S, Hamilton W A and Smith G S 1991 *Physica* B **173** 121
[25] Berk N F and Majkrzak C F 1991 *Phys. Rev.* B **51** 11 296
[26] Iler R K 1979 *The Chemistry of Silica* (New York: Wiley–Interscience)
[27] Kern W 1990 *J. Electrochem. Soc.* **137** 1887
[28] Vig J R 1985 *J. Vac. Sci. Technol.* A **3** 1027
[29] Fragneto G, Thomas R K, Rennie A R and Penfold J 1996 *Langmuir* **12** 6036
[30] Charitat T, Bellet-Amalric E, Fragneto G and Graner F 1999 *Eur. Phys. J.* B **8** 583
[31] Pockels A 1891 *Nature* **43** 437
[32] Sagiv J 1980 *J. Am. Chem. Soc.* **102** 92
[33] Maoz R and Sagiv J 1984 *J. Colloid Interface Sci.* **100** 465
[34] Krueger S, Meuse C W, Majkrzak C F, Dura J A, Berk N F, Tarek M and Plant A L *Langmuir* **17** 511
[35] Porath J 1987 *Biotechnol. Prog.* **3** 14
[36] Boretos J W 1980 *Synthetic Biomedical Polymers: Concepts and Applications* ed M Szycher and W J Robinson (Westport, CT: Technomic)
[37] Dickinson E 1992 *An Introduction to Food Colloids* (Oxford: Oxford University Press)
[38] Horbett T A 1986 *Hydrogels in Medicine and Pharmacy* ed N A Peppas (Boca Raton, FL: Chemical Rubber Company)
[39] Dickinson E, Horne D S, Phipps J S and Richardson R M 1993 *Langmuir* **9** 242
[40] Fragneto G, Thomas R K, Rennie A R and Penfold J 1995 *Science* **267** 657
[41] Su T J, Lu J R, Thomas R K, Cui Z F and Penfold J 1998 *Langmuir* **14** 438
[42] Lipowsky R and Sackmann E 1995 *Structure and Dynamics of Membranes* vol I, parts A and B (Amsterdam: North-Holland–Elsevier)
[43] Sackmann E 1996 *Science* **271** 43
[44] Fragneto G, Graner F, Charitat T, Dubos P and Bellet Amalric E 2000 *Langmuir* **16** 4581
[45] Derossi D, Calvet S, Trembleau A, Brunissen A, Chassaing G and Prochiantz A 1996 *J. Biol. Chem.* **271** 18 188
[46] Brugidou J, Legrand Ch, Méry J and Rabié A 1995 *Biochem. Biophys. Res. Commun.* **214** 685
[47] Tamm L K and McConnell H M 1985 *Biophys. J.* **47** 105
[48] Mora S and Daillant J 2000 private communication
[49] Fragneto G, Charitat T, Graner F, Mecke K, Perino-Gallice L and Bellet-Amalric E 2001 *Europhys. Lett.* **53** 100
[50] Ohki K 1991 *Biochem. Biophys. Res. Commun.* **174** 102
[51] Roser S and Hughes A, private communication
[52] Hughes A V, Goldar A, Gerstenberg M C, Roser S J and Bradshaw J 2001 *Phys. Chem. Chem. Phys.* submitted
[53] Mecke K, Charitat T and Graner F submitted
[54] Fradin C, Luzet D, Braslau A, Alba M, Daillant J, Petit J M and Rieutord F 1998 *Langmuir* **14** 7329